ACS Catalysis

Perspective

pubs.acs.org/acscatalysis

# Artificial Photosynthetic Systems Based on [FeFe]-Hydrogenase Mimics: the Road to High Efficiency for Light-Driven Hydrogen Evolution

Feng Wang, Wen-Guang Wang, Hong-Yan Wang, Gang Si, Chen-Ho Tung, and Li-Zhu Wu*

Key Laboratory of Photochemical Conversion and Optoelectronic Materials, Technical Institute of Physics and Chemistry, The Chinese Academy of Sciences, Beijing 100190, P.R. China

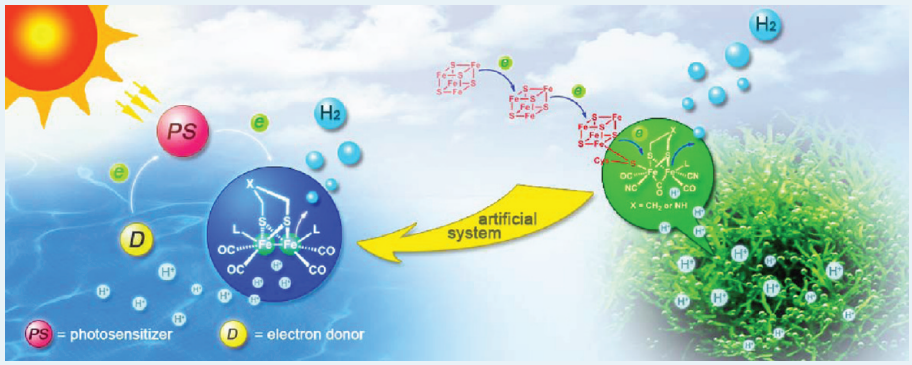


**ABSTRACT:** Hydrogen ($H_2$) has the potential to replace fossil fuels as the clean energy carrier of the future, particularly if it is produced by water splitting using visible light. Natural [FeFe]-hydrogenase ([FeFe]-$H_2$ase) is known to catalyze the reversible reduction of protons to $H_2$ with remarkable activity under mild conditions. In this respect, artificial photosynthetic systems for $H_2$ production by using sunlight and [FeFe]-$H_2$ase mimics have attracted much attention, and great progress has been made in recent years. This perspective paper describes our efforts to achieve $H_2$ evolution by [FeFe]-$H_2$ase mimics powered by a photosensitizer (PS). Covalent-linked molecular dyads and a triad, a self-assembled micelle system and a robust, inexpensive, nanocrystal CdTe system will be highlighted.

**KEYWORDS:** *artificial photosynthesis, [FeFe]-hydrogenase, hydrogen evolution, photocatalyst, photoinduced electron transfer*

## 1. INTRODUCTION

Utilization of sunlight to make fuels represents a promising solution to the looming energy crisis and climate change. Hydrogen ($H_2$) with high specific enthalpy of combustion and benign combustion product (water) is envisaged to be the ideal fuel for reducing mankind's dependence on fossil fuels and subsequent emissions of greenhouse gases.[1−3] Nature long ago figured out how to use a photosynthetic complex to capture sunlight, and then to store its energy in a chemical form, $H_2$, the primary processes of which involve three fundamentals.[3−5] The first is light capture: absorbing the sunlight by chlorophyll. The second is electron transfer: pushing a sunlight-excited electron off its home atom to form spatially separated electron/hole pairs. The third is catalysis: the generated holes are captured by the oxygen-evolving complex to oxidize water ($H_2O$) to oxygen ($O_2$), and the electrons are captured by photosystem I to reduce the proton to $H_2$, or carbon dioxide to carbon fuels. Thus, the overall primary event of photosynthesis is to store solar energy in a fuel by rearranging the chemical bonds of $H_2O$ to form $H_2$ and $O_2$.

Irrespective of $O_2$ evolution, hydrogenases ($H_2$ases), a class of metalloenzymes in certain bacteria and algae, catalyze the reversible reduction of proton and oxidation of $H_2$.[6] Among these distinct $H_2$ases of [Fe]-$H_2$ase, [NiFe]-$H_2$ase, and [FeFe]-$H_2$ase, [FeFe]-$H_2$ase is pretty good at catalyzing the reduction of protons to $H_2$ with turnover rate high up to 6000−9000 $s^{-1}$ under mild conditions (working near the Nernstian potential).[7] X-ray crystallographic analysis revealed that the active center of [FeFe]-$H_2$ase features a butterfly $Fe_2S_2$ subunit coordinated by a cysteine-linked $Fe_4S_4$ cluster, carbon monoxide, and cyanide ligand, and by a dithiolate bridging the two iron centers (Scheme 1).[8,9] The $Fe_2S_2$ subunit serves as the catalytic center for proton reduction, and the $Fe_4S_4$ cluster mediates transfer electron to and from the active site.

The success and importance of photosynthesis have inspired researchers to construct artificial photosynthetic systems for solar energy conversion. Over the past decade, a variety of [FeFe]-$H_2$ase mimics have been shown to function as catalysts for chemical reduction of protons.[10] It has been clear that the electron transfer either electrochemical or photochemical to the $Fe_2S_2$ active site of [FeFe]-$H_2$ase mimics is a prerequisite for $H_2$ evolution.[11−14] From a photochemical point of view, the

Received: September 7, 2011
Revised: January 20, 2012
Published: January 30, 2012

  

**Scheme 1. Active Site of Natural [FeFe]-$H_2$ase**

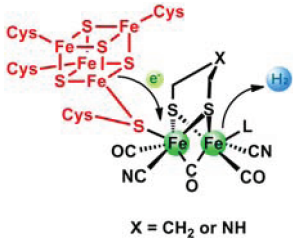


X = $CH_2$ or NH

electron transfer is triggered by a preceding absorption of a photon by a photosensitizer. In general, four components, photosensitizer (PS), $Fe_2S_2$ proton reduction catalyst, and sacrificial electron donor (D) and proton source, are necessary for a photochemical system to accomplish light-driven $H_2$ evolution. No matter how the four components are assembled, the photoexcited PS (PS*) must be quenched either oxidatively or reductively to generate the reduction equivalents by electron transfer. Along this line of consideration, the determination of free energy change ($\Delta G^0$) of the photoinduced electron transfer process is governed by the Rehm–Weller equation (eq 1),[14,15]

$$\Delta G^0 = E_{ox} - E_{red} - E_{00} - C \quad (1)$$

where $E_{ox}$ is the oxidative potential of the species donating an electron, and $E_{red}$ is the reductive potential of the species accepting an electron; $E_{00}$ is the excitation energy of the PS, and $C$ is the sum of solvation effect and the Coulombic energy of the formed iron pair in solution.

In the case of oxidative quenching, the PS* delivers an electron to a $Fe_2S_2$ catalytic center giving rise to $PS^{+\bullet}$ and $Fe_2S_2^{-\bullet}$, that is, the $Fe^IFe^0$ species. The $PS^{+\bullet}$ then reacts with a sacrificial electron donor (D) to regenerate PS. Alternatively, the PS* accepts an electron from a sacrificial electron donor (D), that is, reductive quenching, to form reduced $PS^{-\bullet}$ and oxidized sacrificial electron donor ($D^{+\bullet}$) that is easily degraded. The $PS^{-\bullet}$ subsequently reduces the $Fe_2S_2$ catalytic center in the dark to produce the $Fe^IFe^0$ species. Spectroscopic and electrochemical studies have demonstrated that the $Fe^IFe^0$ species can further react with a proton to generate a $[Fe^IFe^{II}{\cdot}H]$ intermediate for $H_2$ evolution.[11−14]

Since the first attempt by Sun and Åkermark to construct an artificial photocatalytic system for $H_2$ evolution in 2003,[16] extensive studies have been performed focusing on the $Fe_2S_2$ cluster. A summary of the photochemical systems, related to [FeFe]-$H_2$ase mimics for $H_2$ evolution in the literature, is shown in Table 1. It is encouraging to see that the turnover number (TON) of the artificial [FeFe]-$H_2$ase system has been increased from null to more than 500, and the stability under irradiation has been improved from 1 to 10 h. Comprehensive reviews have described both electrochemical and photochemical progress on [FeFe]-$H_2$ase mimics.[14,17−21] Our investigations to achieve light-driven $H_2$ evolution by [FeFe]-$H_2$ase mimics have also been reported in a series of papers.[22−28] In this perspective, we will compile the following four stories to illustrate a few approaches that may be useful in the design of artificial photosynthetic systems for $H_2$ evolution with high efficiency and stability.

(1) $H_2$ evolution by molecular dyads;
(2) $H_2$ evolution by a molecular triad;
(3) $H_2$ evolution from a self-assembling system in an aqueous solution—a biomimetic pathway;
(4) $H_2$ evolution from a robust, inexpensive, nanocrystal CdTe system in water.

## 2. PHOTOCHEMICAL $H_2$ EVOLUTION BY MOLECULAR DYADS BASED ON [FEFE]-$H_2$ASE MIMICS IN HOMOGENEOUS SOLUTION

To make a PS-$Fe_2S_2$ molecular dyad, two different strategies have been put forward (Scheme 2). In the first strategy, the dithiolate-bridge is employed to connect a PS and a $Fe_2S_2$ catalytic center of [FeFe]-$H_2$ase mimics. The second strategy involves anchoring a PS to one of the iron centers of the $Fe_2S_2$ active site. Sun and co-workers reported PS-$Fe_2S_2$ molecular dyads **1** and **2** (Scheme 3) by covalently linking a ruthenium(II) bipyridine

**Table 1. Photochemical Systems Related to [FeFe]-$H_2$ase Mimics for $H_2$ Evolution**

| type | PS | catalyst | proton source | electron donor (D) | solvent | $T_{irr}$[a]/h | TON[b] | ref.[c] |
|---|---|---|---|---|---|---|---|---|
| dyad | **1** | **1** | | | | | 0 | 16 |
| | **2** | **2** | | | | | 0 | 29, 30 |
| | **3** | **3** | | | | | 0 | 31 |
| | **4** | **4** | | | | | 0 | 32 |
| | **5** | **5** | $CF_3COOH$ | ArSH | $CH_2Cl_2$ | 2 | 0.16 | 33 |
| | **6** | **6** | $N^iPr_2EtH{\cdot}OAc$ | $N^iPr_2EtH{\cdot}OAc$ | toluene | 1.3 | 1.96 | 34 |
| | **7** | **7** | $CF_3COOH$ | EtSH | $CH_2Cl_2$ | 1 | 0.31 | 35, 36 |
| | **8** | **8** | $CF_3COOH$ | | toluene | NA[d] | 0.45 | 37 |
| | **9a** | **9a** | $CH_3COOH$ | $CH_3OH$ | $CH_3CN/H_2O$ | 2 | 0.08 | 25 |
| | **9b** | **9b** | $CH_3COOH$ | $CH_3OH$ | $CH_3CN/H_2O$ | 2 | 0.13 | 25 |
| | **9c** | **9c** | $CH_3COOH$ | $CH_3OH$ | $CH_3CN/H_2O$ | 2 | 0.14 | 25 |
| triad | **11a** | **11a** | $H_2A$[e] | $H_2A$ | $CH_3CN$ | 1.5 | 0.35 | 28 |
| multicomponent (micelle) | **12a** | **12c** | $H_2A$[e] | $H_2A$ | $H_2O$ | 2 | 0.13 | 26 |
| | **12a** | **12d** | $H_2A$[e] | $H_2A$ | $H_2O$ | 2 | 0.03 | 26 |
| | **12b** | **12c** | $H_2A$[e] | $H_2A$ | $H_2O$ | 2 | 0.07 | 26 |
| | **12b** | **12d** | $H_2A$[e] | $H_2A$ | $H_2O$ | 2 | 0.04 | 26 |
| multicomponent (organic/water) | $Ru(bpy)_3^{2+}$ | **13** | $H_2A$[e] | $H_2A$ | $CH_3CN/H_2O$ | 3 | 4.3 | 40 |
| | $Ir(ppy)_2(bpy)^+$ | **13** | $H_2O$/TEA[f] | TEA | acetone/$H_2O$ | 8 | 466 | 42 |
| | $Ru(bpy)_3^{2+}$ | **14** | $H_2A$[e] | $H_2A$ | DMF/$H_2O$ | 2.3 | 200 | 41 |
| multicomponent (water) | CdTe QDs | **15** | $H_2A$[e] | $H_2A$ | $H_2O$ | 10 | 505 | 27 |

[a]Irradiation time. [b]Based on $Fe_2S_2$ catalyst. [c]Reference. [d]No available data. [e]Ascorbic acid. [f]Triethylamine.


dx.doi.org/10.1021/cs200458b | ACS Catal. 2012, 2, 407–416

**Scheme 2. Synthetic Strategies to PS-$Fe_2S_2$ Molecular Dyads**

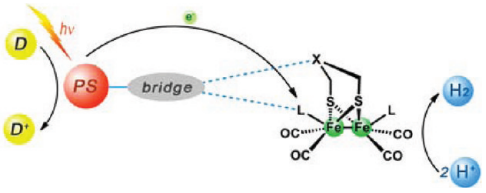


PS to a $Fe_2S_2$ active site of [FeFe]-$H_2$ase mimic.[16,29,30] Later, Song developed dyad **3** by coordinatively linking a zinc porphyrin to a pyridyl modified $Fe_2S_2$ active site.[31] Ott made use of the second approach to synthesize dyad **4** with phenylphosphine-derived ruthenium(II) PS to one of iron centers of the $Fe_2S_2$ active site (Scheme 3).[32] Nevertheless, these dyads were unable to produce $H_2$ photochemically in homogeneous solution (Table 1). Electrochemical and photophysical studies on ruthenium(II) dyads **1**, **2**, and **4** suggested that the reduction potential of the $Fe_2S_2$ active site is more negative than the excited state potential of the ruthenium(II) PS, thus leading to the free energy change of the photoinduced electron transfer positive and photoreduction of the $Fe_2S_2$ catalytic center thermodynamically unfeasible.

Until very recently, photochemical $H_2$ evolution systems based on PS-$Fe_2S_2$ molecular dyads appeared at the forefront (Table 1, Scheme 3). Sun and co-workers assembled the zinc porphyrin PS and the pyridyl-functionalized $Fe_2S_2$ active site to form dyad **5**, and achieved photoinduced $H_2$ evolution with a TON of 0.16.[33] Reek, Hartl, and van Leeuwen linked two different zinc porphyrins to two iron centers in one $Fe_2S_2$ active site by a coordinative bond to afford dyad **6**.[34] Despite of not being entirely understood, $H_2$ could be produced when two different types of zinc-porphyrin PS were present in the solution upon irradiation at $\lambda > 530$ nm (TON = 1.96). In 2009, Song et al. reported that dyad **7** was able to produce $H_2$ under visible light irradiation (TON = 0.31).[35,36] In 2010, Wasielewski and co-workers employed imide as a linkage to bridge zinc porphyrin PS and $Fe_2S_2$ active site.[37] They observed the photoinduced electron transfer from the PS to the $Fe_2S_2$ active site, and obtained $H_2$ by irradiation of a solution containing dyad **8** and $CF_3COOH$.

In the meantime, we have engaged in the investigation of light-driven $H_2$ evolution by [FeFe]-$H_2$ase mimics. Considering that electron transfer is crucial for the realization of $H_2$ evolution, we selected a rhenium(I) polypyridyl complex as a PS because of its powerful redox potential, visible-light absorption,

**Scheme 3. Structure of Previous Reported PS-$Fe_2S_2$ Molecular Dyads 1−8**

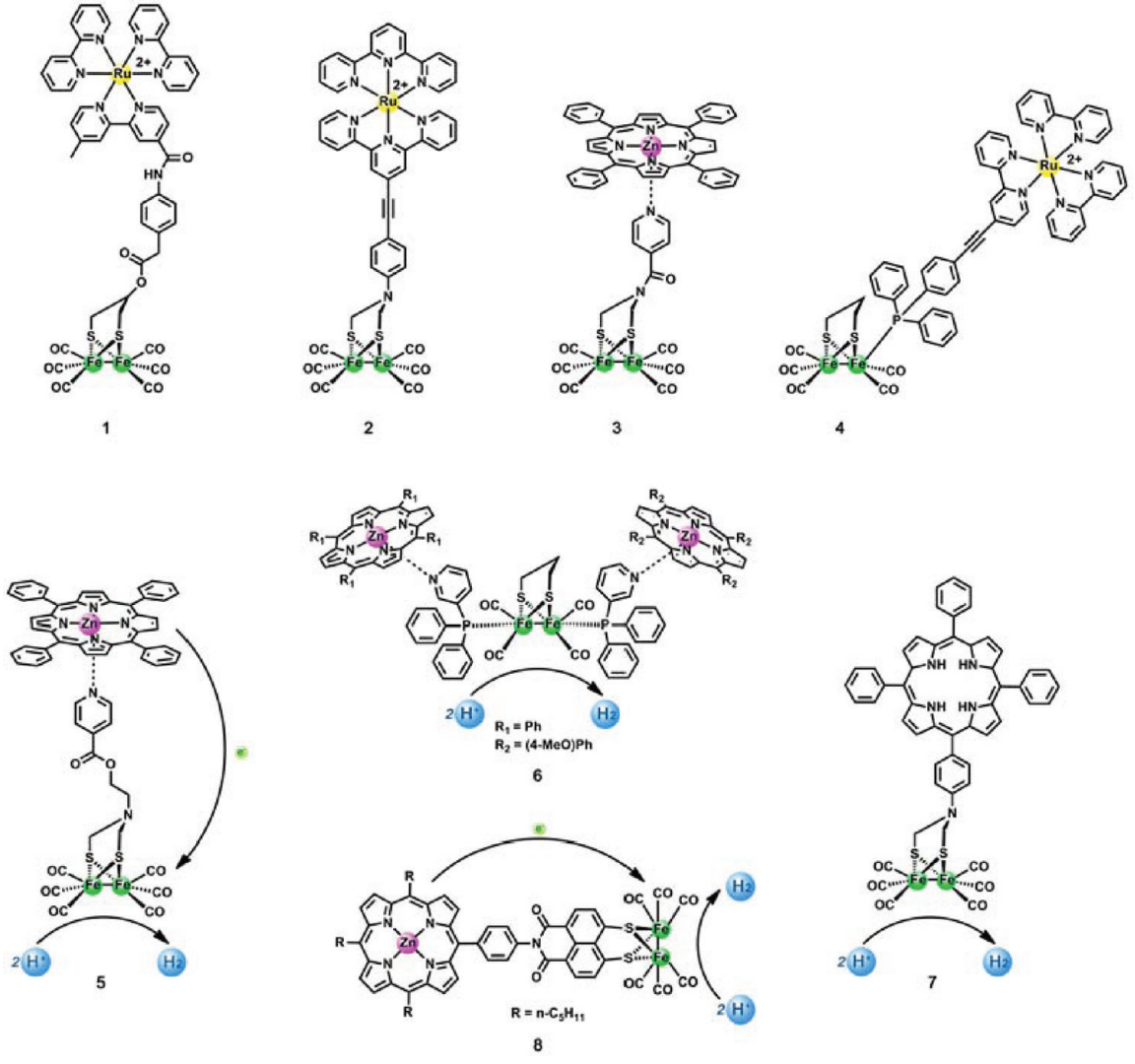



dx.doi.org/10.1021/cs200458b | ACS Catal. 2012, 2, 407−416

**Scheme 4. PS-$Fe_2S_2$ Molecular Dyads 9a−9d and Their References 10a−10c**

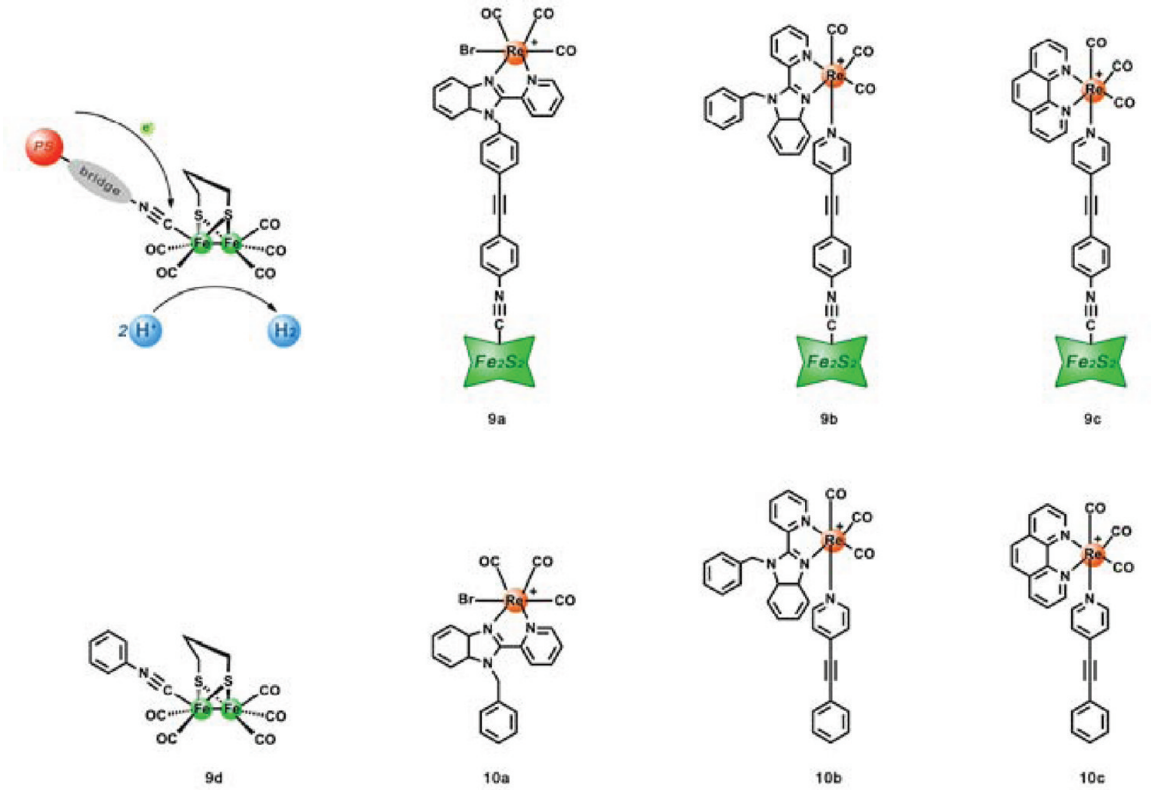


long lifetime of the excited state, and thermal and photochemical stability.[38] An iso-cyanide group was incorporated to anchor the rhenium(I) PS to one of the iron cores of the $Fe_2S_2$ catalytic center affording PS-$Fe_2S_2$ molecular dyads **9a−9c** in reasonable yields (Scheme 4).[25] The linear, rigid, and conjugated bridges were noted to control the separation between PS and $Fe_2S_2$, resulting in the intramolecular electron transfer from the PS* to the $Fe_2S_2$ catalytic site, and the formation of long-lived $Fe^IFe^0$ species. More importantly, molecular dyads **9a−9c** and their intermolecular references **10a**, **10b**, or **10c** with **9d**, respectively, could evolve $H_2$ in degassed mixed solution of $CH_3CN/CH_3OH/H_2O$ under visible light irradiation, in which $CH_3COOH$ was used as proton source and $CH_3OH$ was the sacrificed electron donor. With 1 h of irradiation, the TON of $H_2$ produced from the molecular dyads is more than that of their corresponding intermolecular multicomponent systems under the identical condition (Table 1). The difference in the $H_2$ evolution for **9a**, **9b**, and **9c** implied that the orientation of the rhenium(I) PS, the specific bridge, and the conjugation of the auxiliary ligand play roles in mediating the light-driven $H_2$ production.

The photophysical properties of the PS-$Fe_2S_2$ molecular dyads, together with their reference compounds in $CH_3CN$ solution were examined. The luminescence of **9a−9c** was significantly quenched, but no spectral change could be detected in **10a−10c** when equivalent **9d** was added into the solution under the same condition. Evidently, the intramolecular quenching of the PS* by the $Fe_2S_2$ catalytic center in molecular dyads **9a−9c** operated. The larger quenching extent for **9b** and **9c** than **9a** suggested the more efficient intramolecular quenching of the excited PS by the $Fe_2S_2$ catalytic center. According to the determined oxidation potential $E_{ox}$ of the PS, reduction potential $E_{red}$ of the $Fe_2S_2$ catalytic center, and the excited state energy $E_{00}$ of the PS, the free-energy change shown in Table 2 indicated that the electron transfer process from the excited PS to the $Fe_2S_2$ catalytic center in the designed systems is exothermic. The greater driving force is responsible for the more effective intramolecular electron transfer, and thereby results in the luminescence quenching and photochemical $H_2$ generation with higher efficiency.

Time-resolved absorption spectroscopy (transient absorption spectra) provided direct evidence for the photoinduced electron transfer from the excited PS to the $Fe_2S_2$ catalytic center in these PS-$Fe_2S_2$ molecular dyads. As shown in Figure 1, laser excitation led to a strong transient absorption of the $^3$MLCT state for reference compounds **10a**, **10b**, and **10c** immediately. However, the characteristic absorption of the molecular dyads is quite different from that of **10a**, **10b**, and **10c**, but very similar to the profiles of the $Fe^IFe^0$ species generated by the electrochemical reduction of [FeFe]-$H_2$ase models.[13] The decay of the absorption is monoexponential with a lifetime of 780 $\mu$s for **9a**, and longer than 2 ms for **9b** and **9c** (no decay was observed within instrument limitation of 2 ms). Prolonged irradiation of **9a**, **9b**, and **9c** in $CH_3CN$ solution resulted in no permanent change in their transient absorption spectra, indicating that the $Fe^IFe^0$ species formed by irradiation was stable in the range of microseconds.

On the basis of the above results, it could be speculated that when the PS in the PS-$Fe_2S_2$ molecular dyads is excited, intramolecular electron transfer takes place to generate the reduced $Fe^IFe^0$ species. The greater the driving force is, the more effective the electron-transfer process will be (**9c** > **9b** > **9a**). The generated $Fe^IFe^0$ species is then reacted with a proton to produce a $[Fe^IFe^{II}{\cdot}H]$ intermediate for $H_2$ evolution, and the oxidized $PS^{+\bullet}$ is reduced by accepting an electron from the


dx.doi.org/10.1021/cs200458b | ACS Catal. 2012, 2, 407−416

**Table 2. Electrochemical and Spectroscopic Data of Compounds from Our Laboratory**

| type | system | solvent | $E_{00}$[a]/eV PS | $E_{ox}$[b]/V PS/PS$^+$ | $E_{red}$[b]/V $Fe^IFe^I/Fe^IFe^0$ | $\Delta G^0$/eV | ref.[c] |
|---|---|---|---|---|---|---|---|
| dyads/reference | **9a** | $CH_3CN$ | 2.50 | 0.83 | −1.62 | −0.05[e] | 25 |
| | **9b** | $CH_3CN$ | 2.53 | 0.81 | −1.60 | −0.12[e] | 25 |
| | **9c** | $CH_3CN$ | 2.83 | 0.84 | −1.59 | −0.40[e] | 25 |
| | **10a + 9d** | $CH_3CN$ | 2.50 | 0.83 | −1.58 | −0.09[e] | 25 |
| | **10b + 9d** | $CH_3CN$ | 2.53 | 0.81 | −1.58 | −0.14[e] | 25 |
| | **10c + 9d** | $CH_3CN$ | 2.83 | 0.84 | −1.58 | −0.41[e] | 25 |
| triad/reference | **11a** | $CH_3CN$ | 2.56 | 0.17,[d] 1.03 | −1.49 | −0.90[e] | 28 |
| | **11b + 11c** | $CH_3CN$ | 2.11 | 0.19,[d] 1.04 | −1.57 | −0.80[e] | 28 |
| multicomponent | **12a + 12c** | $H_2O$/SDS[f] | 2.60 | 0.94 | −1.56 | −0.15 | 26 |
| | **12a + 12d** | $H_2O$/SDS[f] | 2.60 | 0.94 | −1.53 | −0.18 | 26 |
| | **12b + 12c** | $H_2O$/SDS[f] | 2.53 | 0.97 | −1.58 | −0.05 | 26 |
| | **12b + 12d** | $H_2O$/SDS[f] | 2.53 | 0.97 | −1.53 | −0.08 | 26 |
| | **15 + CdTe QDs** | $H_2O$ | 1.84[g] | −0.31 | −1.28 | −0.87[e] | 27 |

[a]The excited state energy $E_{00}$ was calculated by using the intersection between emission and excitation spectra. [b]All potentials versus $Fc/Fc^+$. [c]Reference. [d]The oxidative potential of $Fc/Fc^+$ in triad **11a** and dyad **11b**. [e]The $\Delta G^0$ is determined by a simplified Rehm−Weller equation $\Delta G^0 = E_{ox} - E_{red} - E_{00}$. [f]Sodium dodecyl sulfate (SDS) micelle aqueous solution. [g]The excited state energy $E_{00}$ was determined by using the maximum of the CdTe QDs emission at pH 4.0.

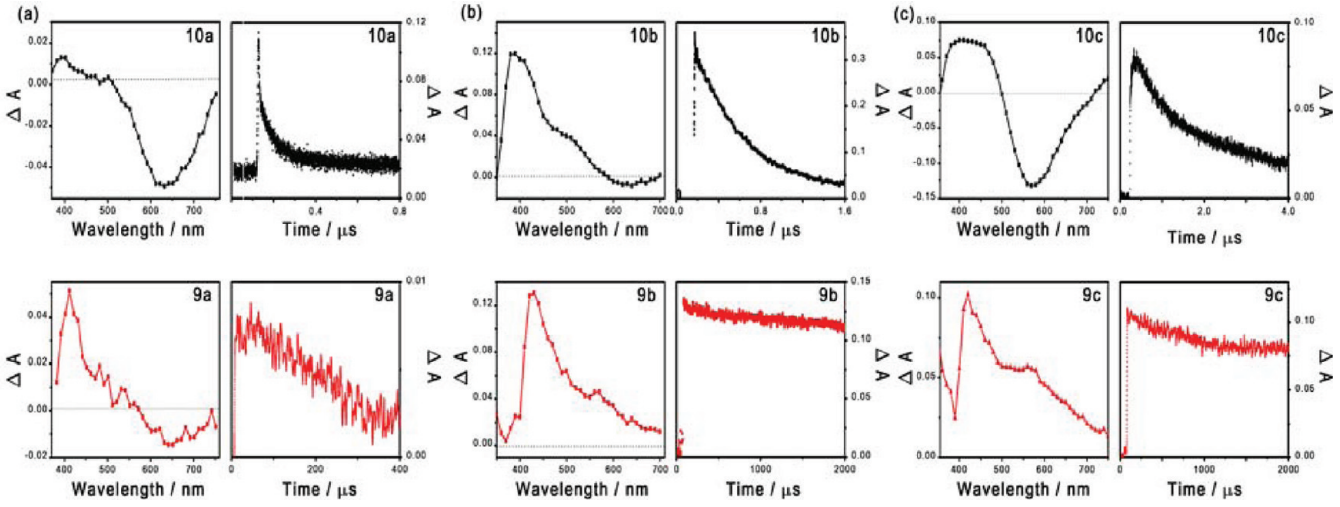


**Figure 1.** Transient absorption spectra and the corresponding kinetic traces of (a) **9a** and **10a**; (b) **9b** and **10b**; (c) **9c** and **10c** upon laser pulse by 355 nm light in $CH_3CN$ under argon atmosphere. The kinetic trace recorded at 390 nm for **10a** and 410 nm for **9a**; 390 nm for **10b** and 430 nm for **9b**; 395 nm for **10c** and 420 nm for **9c**, respectively.

sacrificial electron donor (D) to get back to the ground state (Scheme 5). The orientation of the PS and the specific linkage in PS-$Fe_2S_2$ molecular dyads **9a**, **9b** and **9c** were found important for the formation of the $Fe^IFe^0$ species. The unprecedented long-lived $Fe^IFe^0$ species in the PS-$Fe_2S_2$ molecular dyads is believed to be responsible for the performance on photochemical $H_2$ production.

## 3. PHOTOCHEMICAL $H_2$ EVOLUTION BY A MOLECULAR TRIAD BASED ON [FEFE]-$H_2$ASE MIMIC IN HOMOGENEOUS SOLUTION

Photosynthesis in nature provides a blueprint for the conversion of sunlight to chemical energy by a chain of photoinduced electron transfer processes.[4−6] [FeFe]-$H_2$ase can couple to the electron transfer events and catalyze the reversible reduction of protons to $H_2$ with remarkable activity. In an effort to develop artificial molecular systems, we made a rigid molecular triad **11a** by using a ferrocene as a potential electron donor, a rhenium(I) complex as the PS and a $Fe_2S_2$ cluster as the catalyst (Scheme 6).[28] The assembly of the electron donor, the PS, and the $Fe_2S_2$ catalytic center of [FeFe]-$H_2$ase mimic provided more powerful driving force for the photoinduced electron transfer than those dyads discussed above,[25,33−37] and at the same time the long

**Scheme 5. Proposed Photophysical Pathway for PS-$Fe_2S_2$ Molecular Dyads**

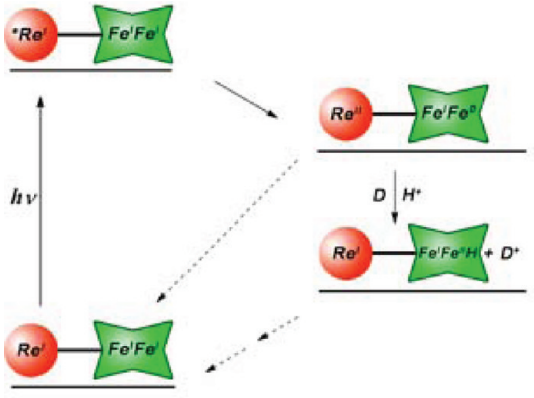



dx.doi.org/10.1021/cs200458b | ACS Catal. 2012, 2, 407−416

**Scheme 6. Molecular Triad 11a and Its Reference Compounds 11b and 11c**

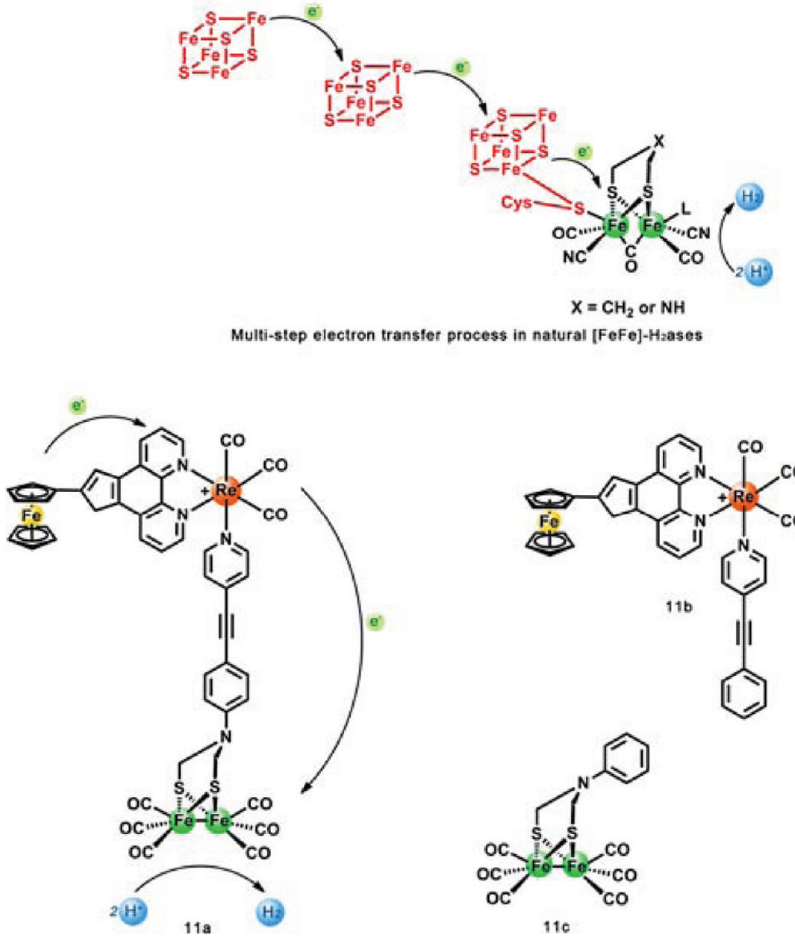


distance and weak electronic coupling between the terminal donor and the $Fe_2S_2$ catalytic center in triad **11a** inhibited charge recombination, which is reminiscent of the multistep photoinduced electron transfer employed to achieve long-lived charge separation in natural photosynthesis.

Triad **11a** and its reference compound **11b** are not emissive in solution at room temperature. With the addition of an oxidant into the solution, the typical emission of rhenium(I) complex **11b** was enhanced greatly. However, its absorption in the low-energy region remained unchanged. The results indicated that the rhenium(I) PS and the ferrocene donor in **11b** interacted weakly in the ground state, but such interaction did occur in the excited state. The oxidation of the ferrocene restored the emission capability of the rhenium(I) PS by preventing photoinduced electron transfer from the ferrocene donor to the rhenium(I) PS in complex **11b**. In sharp contrast, with the titration of the oxidant into the solution of triad **11a** under the same condition, not much spectral change implied that the intramolecular quenching of the revived PS by the $Fe_2S_2$ catalytic center in triad **11a** operated.

Combining electrochemical and spectroscopic studies, we estimated the free energy change of triad **11a**, and **11b** with **11c**, respectively (Table 2). The results demonstrated that the photoinduced electron transfer in the designed system is thermodynamically favorable. More interestingly, information on the electron transfer dynamics was obtained from their time-resolved absorption spectra (Figure 2). The kinetics probed at 400 nm of **11b** showed a fast rise phase followed by a slow decay (Figure 2c). The rise suggests the formation of charge-separated state in **11b** with forward electron transfer rate constant of $1.09 \times 10^6$ $s^{-1}$, while the decay represents the recombination of charge-separated state with back electron transfer rate constant of $1.75 \times 10^5$ $s^{-1}$ (5.7 $\mu$s) at room temperature. When [FeFe]-$H_2$ase mimic **11c** was introduced, a series of new absorptions of **11b** at around 400 nm appeared immediately (Figure 2b). The new absorption was weak, but its shape was similar to that of triad **11a**, both of which are in line with that of the $Fe^IFe^0$ species formed by electrochemical reduction of [FeFe]-$H_2$ase mimics.[13] The decays of the $Fe^IFe^0$ absorptions could be described by a monoexponential function with a lifetime of 708 $\mu$s for **11b** with **11c**, and >2 ms for triad **11a**, respectively (Figure 2d–e).

Evidently, triad **11a** yielded much more and longer-lived $Fe^IFe^0$ species than the combined **11b** and **11c** under the same concentration, which was anticipated to make more contribution to the light-driven $H_2$ generation. As expected, the photochemical $H_2$ evolution experiments showed that triad **11a** generated more $H_2$ (TON = 0.35) than the corresponding system of **11b** with **11c** (TON = 0.04) at the same condition. Although the light-driven reaction was not catalytic yet, the combination of the ferrocene donor, the rhenium(I) PS, and the [FeFe]-$H_2$ase mimic was found helpful in improving the performance of light-driven $H_2$ evolution. The difference in the $H_2$ evolution efficiency for triad **11a**, and **11b** with **11c** implied that the assembly of an electron donor, a chromophore and


dx.doi.org/10.1021/cs200458b | ACS Catal. 2012, 2, 407–416

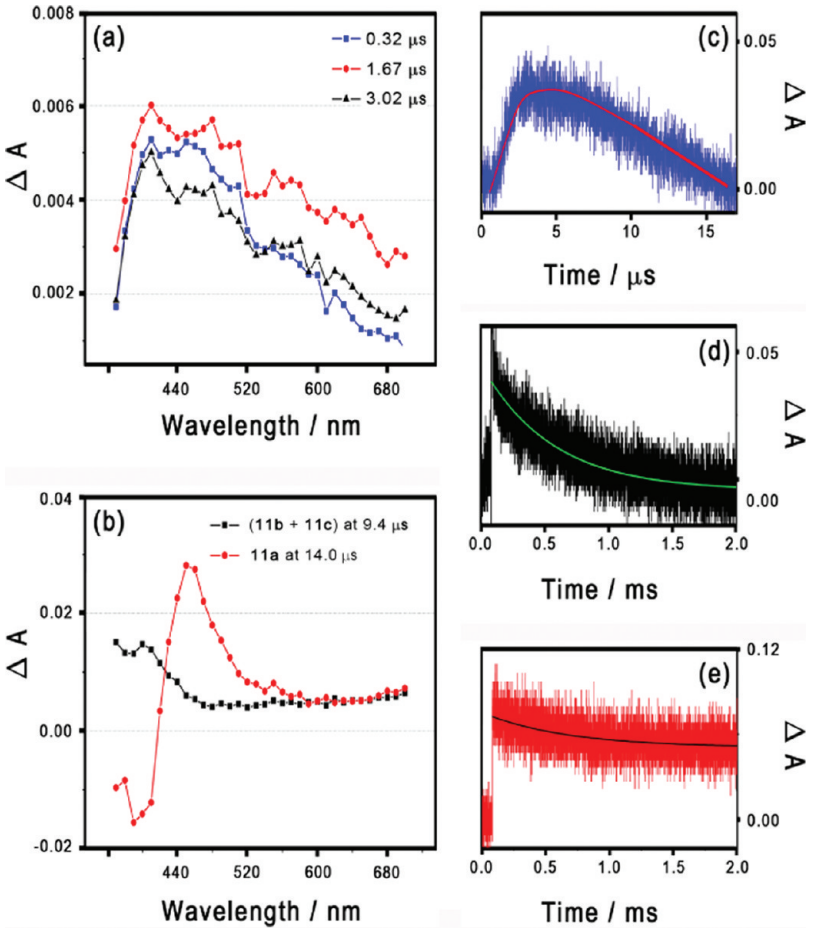


**Figure 2.** Transient absorption spectra of (a) **11b** and (b) triad **11a** (red), **11b** with **11c** (black); the kinetic trace recorded at (c) 400 nm for **11b**; (d) 400 nm for **11b** with **11c**; (e) 440 nm for triad **11a** upon laser pulse by 355 nm light in $CH_3CN$ under argon atmosphere.

[FeFe]-$H_2$ase mimic to build up a multistep photoinduced electron transfer chain is a promising strategy for $H_2$ evolution.

## 4. PHOTOCHEMICAL $H_2$ EVOLUTION FROM A SELF-ASSEMBLING SYSTEM IN AN AQUEOUS SOLUTION: A BIOMIMETIC PATHWAY

Enzymes may bind substrates in elaborate pockets to direct a specific reaction pathway under mild conditions. [FeFe]-$H_2$ase is deeply embedded within the protein matrix to operate the reversible reduction of protons to $H_2$ with remarkable activity.[6,7] Developing a new system capable of simulating the functionality of [FeFe]-$H_2$ase under aqueous conditions becomes an important objective to pursue.

Micelles have long been used to simulate a water-membrane interface found in biological systems. Like a cell membrane to some extent, it contains a negatively charged surface and a hydrophobic interior in water. We employed one of the most popular micelles, sodium dodecyl sulfate (SDS) micelle, to incorporate rhenium(I) PS **12a** or **12b** and $Fe_2S_2$ catalysts of [FeFe]-$H_2$ase mimic **12c** or **12d** in water, where ascorbic acid ($H_2A$) was used as a sacrificial electron donor and proton source (Scheme 7).[26] The assembly of the active components increased their solubility in water, and realized $H_2$ evolution in an aqueous solution by visible light irradiation. With respect to the subtle changes in the molecular structure of PS and $Fe_2S_2$ catalytic centers, spectroscopic study and $H_2$ generation provided valuable information on the extent they are included into the SDS micelle that is reminiscent of [FeFe]-$H_2$ase enzymes buried in a protein matrix.

The interaction of the SDS micelles with the PS and $Fe_2S_2$ catalysts in water was clearly observed, suggesting that the water-insoluble PS and $Fe_2S_2$ catalysts were incorporated into the SDS micelle solution and the extent of the incorporation was selective. When the aqueous SDS micelle solution was irradiated for 1 h ($\lambda$ > 400 nm), the amount of $H_2$ evolution from the mixture of **12a** and **12c** was much higher than that from the mixture of **12a** and **12d**, **12b** and **12c**, **12b** and **12d**, respectively (Table 1). Because the concentration of each complex included in the SDS micelle solution was different, we performed the reaction of the mixtures of **12a** and **12c**, **12b** and **12c** at identical concentration for systematic comparison. Notably, the amount of $H_2$ evolution from the mixture of **12a** and **12c** was still higher than that of **12b** and **12c**. As the extinction coefficients above $\lambda$ > 400 nm for **12a** and **12b** were identical in both cases, and the higher concentration of **12a** and **12c** included in the SDS micelle bore higher efficiency, the strong interaction and close contact between the excited PS and the $Fe_2S_2$ catalysts are believed crucial for the efficient $H_2$ generation with visible light irradiation.

Although three-component intermolecular systems containing a ruthenium(II) or iridium(III) PS, a [FeFe]-$H_2$ase mimic like **13** or **14** (Scheme 8), and a sacrificial electron donor have been extensively studied since the first report in 2008,[39−42] it is rather difficult to conduct such reactions in water because neither PS nor $Fe_2S_2$ catalyst of [FeFe]-$H_2$ase mimic is water-soluble.


dx.doi.org/10.1021/cs200458b | *ACS Catal.* 2012, 2, 407−416

**Scheme 7. Photochemical $H_2$ Evolution from an Aqueous SDS Micelle Solution**

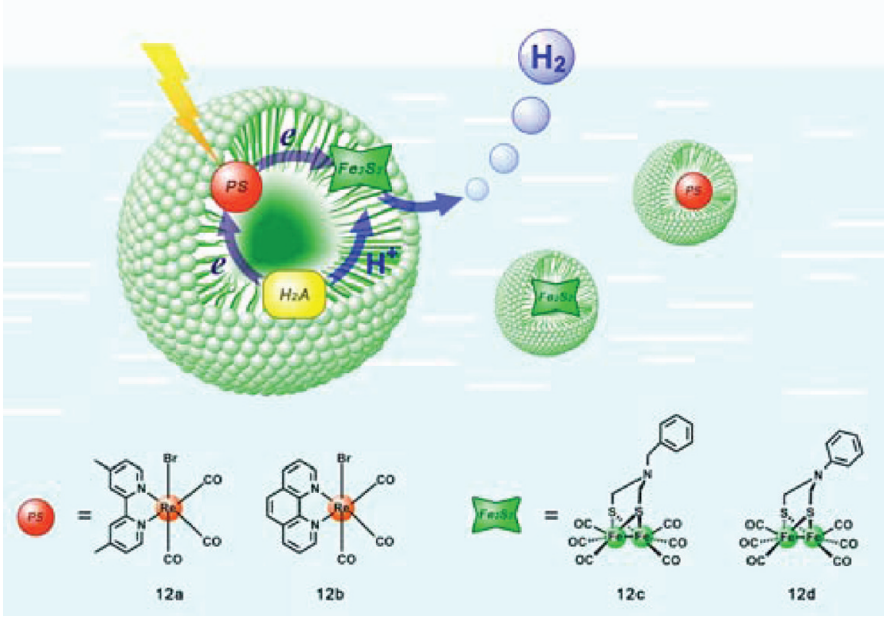


**Scheme 8. [FeFe]-$H_2$ase Mimics 13 and 14 Studied in Multi-Component Systems**

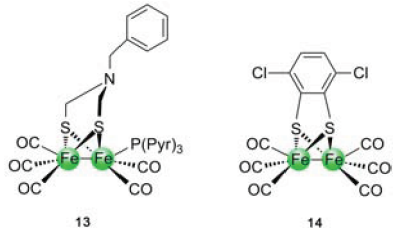


Furthermore, the excited PS is not sufficient to deliver an electron to the $Fe_2S_2$ catalyst in the previous three-component systems. However, the potential of rhenium(I) PS is on the contrary. From estimation of the free energy change (Table 2) and analysis of the kinetics, we considered that the electron transfer process from the excited rhenium(I) PS to the $Fe_2S_2$ catalysts occurred, and thereby gave rise to $Fe^IFe^0$ species. The better performance for **12a** and **12c** than **12b** and **12c** implied that both the driving force for the photoinduced electron transfer and the close contact between the excited PS and the $Fe_2S_2$ catalysts are advantageous.

## 5. PHOTOCATALYTIC $H_2$ EVOLUTION FROM A ROBUST, INEXPENSIVE, NANOCRYSTAL CDTE SYSTEM IN WATER

In comparison to the efficient [FeFe]-$H_2$ase in nature, however, artificial photosynthetic systems thus far give rise to a small amount of $H_2$ upon irradiation, and finally finish their photochemical $H_2$ evolution in an organic solution or a mixture of organic solvents and water. More strikingly, the synthetic [FeFe]-$H_2$ase mimics are not stable and easily decompose generally within 1 h of irradiation. Very recently, we constructed an efficient photocatalytic system for $H_2$ evolution in aqueous solution (Scheme 9),[27] where an iso-cyanide group was used to link three hydrophilic ether chains to the $Fe_2S_2$ active site of the [FeFe]-$H_2$ase mimic so as to improve the solubility of the $Fe_2S_2$ catalyst **15** in water. Nanocrystal CdTe

**Scheme 9. Artificial System for Photocatalytic $H_2$ Evolution Based on $Fe_2S_2$ Catalyst 15 and Nanocrystal MPA-CdTe**

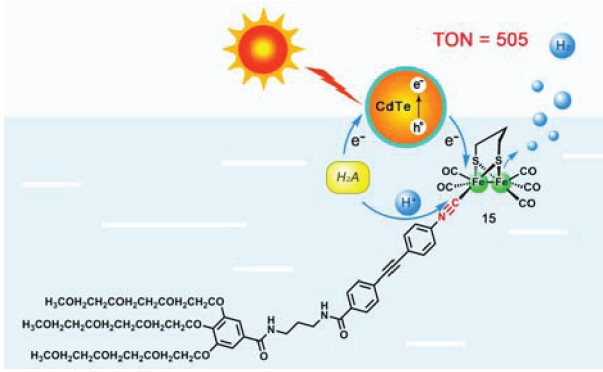


stabilized by 3-mercapto-propionic acid (MPA-CdTe) was selected as a PS on account of its broad visible-light absorption, aqueous dispersion, and economical advantage over a precious metal PS.[43−45] $H_2A$, used as a proton source and a sacrificial electron donor, is water-soluble and thus allows for the incorporation of a large amount of $H_2A$ in the reaction vessel.

The rate of $H_2$ evolution was found dependent on the pH of the solution, and the concentration of the MPA-CdTe and $H_2A$. Under optimized condition, more than 500 equiv of $H_2$ per $Fe_2S_2$ catalyst **15** were achieved with 10 h of irradiation, indicating that both $Fe_2S_2$ catalyst **15** and the MPA-CdTe are regenerated in the whole photocatalytic reaction. The catalytic activity and stability are the highest known to date for light-driven $H_2$ production by artificial [FeFe]-$H_2$ase mimics.

The photoinduced electron transfer from the MPA-CdTe PS to the $Fe_2S_2$ catalyst **15** was confirmed by the evaluation of the free-energy change and $Fe^IFe^0$ species. Although the excited MPA-CdTe was capable of both oxidatively and reductively quenching by $Fe_2S_2$ catalyst **15** and $H_2A$, the relative quenching extent and rate constant indicated that oxidative quenching by $Fe_2S_2$ catalyst **15** dominated. The reduced $Fe_2S_2$ catalytic center **15**, $Fe^IFe^0$ species, could further react with a proton for $H_2$


dx.doi.org/10.1021/cs200458b | ACS Catal. 2012, 2, 407−416

evolution. On the other hand, the formed hole remaining in the MPA-CdTe after electron transfer was subsequently regenerated by the sacrificial electron donor $H_2A$. As two electrons are required to produce each molecule of $H_2$, the consecutive two-electron oxidation of $H_2A$ must be responsible for the regeneration of MPA-CdTe and $Fe_2S_2$ catalyst **15**.

## 6. CONCLUSION AND OUTLOOK

We have shown several artificial photosynthetic systems based on [FeFe]-$H_2$ase mimics for $H_2$ evolution. (1) Three molecular dyads bearing a rhenium(I) PS directly linked to one of iron centers of $Fe_2S_2$ active site of [FeFe]-$H_2$ase mimics, and one triad assembling an electron donor, a rhenium(I) PS and a $Fe_2S_2$ catalytic center, have been successfully constructed. Time-dependence of $H_2$ evolution and spectroscopic study clearly demonstrate that the larger driving force of the photoinduced electron transfer from the PS to the $Fe_2S_2$ catalytic center, and the longer lifetime of $Fe^IFe^0$ species of the reduced $Fe_2S_2$ catalytic center, are important for $H_2$ evolution by visible light. (2) Self-assembly approach has been employed to mimic natural [FeFe]-$H_2$ase. Studies on the efficiency of photochemical $H_2$ production reveal that the strong interaction and close contact of the excited PS and $Fe_2S_2$ active site of [FeFe]-$H_2$ase mimics are crucial for $H_2$ evolution in an aqueous SDS micelle solution. This finding may be helpful in understanding the activity and mechanism of the catalytic cluster where in nature it is buried in a protein matrix. (3) A robust, inexpensive, nanocrystal CdTe system for photocatalytic $H_2$ production in water has been achieved. The obtained TON (505) is competitive with those from current state-of-the-art catalytic systems for $H_2$ production. The result shows that a synthetic $Fe_2S_2$ catalytic center of [FeFe]-$H_2$ase mimics, even the most popular type one that would decompose generally in 1 h irradiation, can act as an effective catalyst for light-driven $H_2$ production.

For the purpose of solar fuel $H_2$ production, these artificial systems offer a shortcut to taking advantage of the efficient principles of the primary photosynthetic reaction. The greater diversity in molecular design and the smaller components than their natural counterparts in artificial systems have higher potential for $H_2$ production. Photochemical methods coupled with time-resolved spectroscopy provide unique opportunities to identify and monitor intermediates in the reaction cycle leading to $H_2$ evolution. The kinetics measurements can shed more light on rate-limiting processes and the mechanism as a whole. At present, this field is so active that we have every reason to believe that scientists will soon be able to design and construct artificial [FeFe]-$H_2$ase systems for $H_2$ production with higher efficiency.

## AUTHOR INFORMATION

### Corresponding Author

*E-mail: lzwu@mail.ipc.ac.cn.

### Funding

We are grateful for financial support from the Ministry of Science and Technology of China (2009CB22008, and 2007CB808004), the National Science Foundation of China (50973125, 21090343, and 20732007), Solar Energy Initiative of the Knowledge Innovation Program of the Chinese Academy of Sciences (KGCXZ-YW-389), and the Bureau for Basic Research of the Chinese Academy of Sciences.

### Notes

The authors declare no competing financial interest.

## REFERENCES

(1) Gray, H. B. *Nat. Chem.* **2009**, *1*, 7.
(2) Esswein, A. J.; Nocera, D. G. *Chem. Rev.* **2007**, *107*, 4022−4047.
(3) Barber, J. *Chem. Soc. Rev.* **2009**, *38*, 185−196.
(4) Lubitz, W.; Reijerse, E. J.; Messinger, J. *Energy Environ. Sci.* **2008**, *1*, 15−31.
(5) Magnuson, A.; Anderlund, M.; Johansson, O.; Lindblad, P.; Lomoth, R.; Polivka, T.; Ott, S.; Stensjö, K.; Styring, S.; Sundström, V.; Hammarström, L. *Acc. Chem. Res.* **2009**, *42*, 1899−1909.
(6) Ghirardi, M. L.; Dubini, A.; Yu, J.; Maness, P.-C. *Chem. Soc. Rev.* **2009**, *38*, 52−61.
(7) Frey, M. *ChemBioChem* **2002**, *3*, 153−160.
(8) Adams, M. W. W.; Stiefel, E. I. *Science* **1998**, *282*, 1842−1843.
(9) Cammack, R. *Nature* **1999**, *397*, 214−215.
(10) Tard, C.; Pickett, C. J. *Chem. Rev.* **2009**, *109*, 2245−2274.
(11) Chong, D.; Georgakaiki, I. P.; Mejia-Rodriguez, R.; Sanabria-Chinchilla, J.; Soriaga, M. P.; Darensbourg, M. Y. *Dalton Trans.* **2003**, 4158−4163.
(12) Mejia-Rodriguez, R.; Chong, D.; Reibenspies, J. H.; Soriaga, M. P.; Darensbourg, M. Y. *J. Am. Chem. Soc.* **2004**, *126*, 12004−12014.
(13) Borg, S. J.; Behrsing, T.; Best, S. P.; Razavet, M.; Liu, X.; Pickett, C. J. *J. Am. Chem. Soc.* **2004**, *126*, 16988−16999.
(14) Lomoth, R.; Ott, S. *Dalton Trans.* **2009**, 9952−9959.
(15) Rehm, D.; Weller, A. *Isr. J. Chem.* **1970**, *8*, 259−271.
(16) Wolpher, H.; Borgström, M.; Hammarström, L.; Bergquist, J.; Sundström, V.; Styring, S.; Sun, L.; Åkermark, B. *Inorg. Chem. Commun.* **2003**, *6*, 989−991.
(17) Gloaguen, F.; Rauchfuss, T. B. *Chem. Soc. Rev.* **2009**, *38*, 100−108.
(18) Capon, J.-F.; Gloaguen, F.; Pétillon, F. Y.; Schollhammer, P.; Talarmin, J. *Coord. Chem. Rev.* **2009**, *253*, 1476−1494.
(19) Wang, M.; Na, Y.; Gorlov, M.; Sun, L. *Dalton Trans.* **2009**, 6458−6467.
(20) Wang, M.; Sun, L. *ChemSusChem* **2010**, *3*, 551−554.
(21) Reisner, E. *Eur. J. Inorg. Chem.* **2011**, 1005−1016.
(22) Si, G.; Wu, L.-Z.; Wang, W.-G.; Ding, J.; Shan, X.-F.; Zhao, Y.-P.; Tung, C.-H.; Xu, M. *Tetrahedron Lett.* **2007**, *48*, 4775−4779.
(23) Si, G.; Wang, W.-G.; Wang, H.-Y.; Tung, C.-H.; Wu, L.-Z. *Inorg. Chem.* **2008**, *47*, 8101−8111.
(24) Wang, W.-G.; Wang, H.-Y.; Si, G.; Tung, C.-H.; Wu, L.-Z. *Dalton Trans.* **2009**, 2712−2720.
(25) Wang, W.-G.; Wang, F.; Wang, H.-Y.; Si, G.; Tung, C.-H.; Wu, L.-Z. *Chem.—Asian J.* **2010**, *5*, 1796−1803.
(26) Wang, H.-Y.; Wang, W.-G.; Si, G.; Wang, F.; Tung, C.-H.; Wu, L.-Z. *Langmuir* **2010**, *26*, 9766−9771.
(27) Wang, F.; Wang, W.-G.; Wang, X.-J.; Wang, H.-Y.; Tung, C.-H.; Wu, L.-Z. *Angew. Chem., Int. Ed.* **2011**, *50*, 3193−3197.
(28) Wang, H.-Y.; Si, G.; Cao, W.-N.; Wang, W.-G.; Li, Z.-J.; Wang, F.; Tung, C.-H.; Wu, L.-Z. *Chem. Commun.* **2011**, *47*, 8406−8408.
(29) Ott, S.; Kritikos, M.; Åkermark, B.; Sun, L. *Angew. Chem., Int. Ed.* **2003**, *42*, 3285−3288.
(30) Ott., S.; Borgström, M.; Kritikos, M.; Lomoth, R.; Bergquist, J.; Åkermark, B.; Hammarström, L.; Sun, L. *Inorg. Chem.* **2004**, *43*, 4683−4692.
(31) Song, L.-C.; Tang, M.-Y.; Mei, S.-Z.; Huang, J.-H.; Hu, Q.-M. *Organometallics* **2007**, *26*, 1575−1577.
(32) Ekström, J.; Abrahamsson, M.; Olson, C.; Bergquist, J.; Kaynak, F. B.; Eriksson, L.; Sun, L.-C.; Becker, H.-C.; Åkermark, B.; Hammarström, L.; Ott, S. *Dalton Trans.* **2006**, 4599−4606.
(33) Li, X.; Wang, M.; Zhang, S.; Pan, J.; Na, Y.; Liu, J.; Åkermark, B.; Sun, L. *J. Phys. Chem. B.* **2008**, *112*, 8198−8202.
(34) Kluwer, A. M.; Kapre, R.; Hartl, F.; Lutz, M.; Spek, A. L.; Brouwer, A. M.; van Leeuwen, P. W. N. M.; Reek, J. N. H. *Proc. Natl. Acad. Sci. U.S.A.* **2009**, *106*, 10460−10465.
(35) Song, L.-C.; Tang, M.-Y.; Su, F.-H.; Hu, Q.-M. *Angew. Chem., Int. Ed.* **2006**, *45*, 1130−1133.
(36) Song, L.-C.; Wang, L.-X.; Tang, M.-Y.; Li, C.-G.; Song, H.-B.; Hu, Q.-M. *Organometallics* **2009**, *28*, 3834−3841.

(37) Samuel, A. P. S.; Co, D. T.; Stern, C. L.; Wasielewski, M. R. *J. Am. Chem. Soc.* **2010**, *132*, 8813−8815.
(38) Schanze, K. S.; MacQueen, D. B.; Perkins, T. A.; Cabana, L. A. *Coord. Chem. Rev.* **1993**, *112*, 63−89.
(39) Na, Y.; Zhang, P.; Wang, M.; Sun, L. *Inorg. Chem.* **2007**, *46*, 3813−3815.
(40) Na, Y.; Wang, M.; Pan, J.-X.; Zhang, P.; Åkermark, B.; Sun, L. *Inorg. Chem.* **2008**, *47*, 2805−2810.
(41) Streich, D.; Astuti, Y.; Orlandi, M.; Schwartz, L.; Lomoth, R.; Hammarström, L.; Ott, S. *Chem.—Eur. J.* **2010**, *16*, 60−63.
(42) Zhang, P.; Wang, M.; Na, Y.; Li, X.; Jiang, Y.; Sun, L. *Dalton Trans.* **2010**, *39*, 1204−1206.
(43) Li, Y.; Jing, L.; Qiao, R.; Gao, M. *Chem. Commun.* **2011**, *47*, 9293−9311.
(44) Brown, K. A.; Dayal, S.; Ai, X.; Rumbles, G.; King, P. W. *J. Am. Chem. Soc.* **2010**, *132*, 9672−9680.
(45) Nann, T.; Ibrahim, S. K.; Woi, P.-M.; Xu, S.; Ziegler, J.; Pickett, C. J. *Angew. Chem., Int. Ed.* **2010**, *49*, 1574−1577.